

# THE ORIGIN OF C IV ABSORPTION SYSTEMS AT REDSHIFTS $z < 1$ —DISCOVERY OF EXTENDED C IV ENVELOPES AROUND GALAXIES<sup>1</sup>

HSIAO-WEN CHEN<sup>2</sup> and KENNETH M. LANZETTA

Department of Physics and Astronomy, State University of New York at Stony Brook  
Stony Brook, NY 11794–3800, U.S.A.  
lanzetta@sbastr.ess.sunysb.edu

and

JOHN K. WEBB

School of Physics, University of New South Wales  
Sydney 2052, NSW, AUSTRALIA  
jkw@edwin.phys.unsw.edu.au

---

<sup>1</sup>Based on observations with the NASA/ESA Hubble Space Telescope, obtained at the Space Telescope Science Institute, which is operated by the Association of Universities for Research in Astronomy, Inc., under NASA contract NAS5–26555.

<sup>2</sup>Current address: Observatories of the Carnegie Institution of Washington, 813 Santa Barbara Street, Pasadena, CA 91101, U.S.A. E-Mail: hchen@ociw.edu

## ABSTRACT

We report the discovery of extended C IV gaseous envelopes around galaxies of a wide range of luminosity and morphological type. First, we show that C IV absorption systems are strongly clustered around galaxies on velocity scales of  $v \lesssim 250 \text{ km s}^{-1}$  and impact parameter scales of  $\rho \lesssim 100 h^{-1} \text{ kpc}$  but not on larger velocity or impact parameter scales. Next, adopting measurements of galaxy properties presented in previous papers (which include  $B$ -band luminosity, surface brightness, and disk-to-bulge ratio), we examine how properties of the C IV absorption systems depend on properties of the galaxies. On the basis of 14 galaxy and absorber pairs and 36 galaxies that do not produce corresponding C IV absorption lines to within sensitive upper limits, we find that: (1) Galaxies of a range of morphological type and luminosity appear to possess extended C IV gaseous envelopes of radius  $R \approx 100 h^{-1} \text{ kpc}$ , with abrupt boundaries between the C IV absorbing and non-absorbing regions. (2) The extent of C IV-absorbing gas around galaxies scales with galaxy  $B$ -band luminosity as  $R \propto L_B^{0.5 \pm 0.1}$  but does not depend strongly on galaxy surface brightness, redshift, or morphological type. And (3) the covering factor of C IV clouds within  $\approx 100 h^{-1} \text{ kpc}$  of galaxies is nearly unity, but there is a large scatter in the mean number of clouds encountered along the line of sight. After scaling to the luminosity of an  $L_*$  galaxy, we find that 13 of 14 galaxies of impact parameter  $\rho < 100 h^{-1} \text{ kpc}$  are associated with corresponding C IV absorption lines, while only one of 36 galaxies of impact parameter  $\rho > 100 h^{-1} \text{ kpc}$  are associated with corresponding C IV absorption lines. The most significant implication of the study is that galaxies of a wide range of luminosity and morphological type are surrounded by chemically enriched gas that extends for at least  $\approx 100 h^{-1} \text{ kpc}$ . We consider various scenarios that may have produced metals at large galactic distance and conclude that accreting satellites are most likely to be responsible for chemically enriched gas at large galactic distances to regular looking galaxies.

*Subject headings:* galaxies: evolution—quasars: absorption lines

## 1. INTRODUCTION

Metal-line absorption systems observed in the spectra of background QSOs provide a unique probe of the chemical content and dynamics of gas at large galactic distances. Comparison of galaxies and Mg II absorption systems along common lines of sight has demonstrated that (1) Mg II absorption systems arise in extended gaseous envelopes of galaxies and (2) the gaseous extent of galaxies (at very low column densities) stretches for many times the optical extent of galaxies (Bergeron & Boissé 1991; Lanzetta & Bowen 1990, 1992; Steidel 1993). But while occasional galaxies associated with C IV absorption systems have been reported by various authors (Bergeron et al. 1994; Lanzetta et al. 1995; Steidel et al. 1997; Churchill et al. 1999), no uniform sample of galaxies and C IV absorption systems has yet been applied to systematically investigate statistical properties of extended C IV-absorbing gas around galaxies. In contrast to Mg II absorption systems, C IV absorption systems probe highly-ionized, low-density regions (Wolfe 1983; Bergeron & Stasińska 1986), which suggests that gas traced by C IV is typically at much larger galactic distances than gas traced by Mg II. Hence C IV absorption systems may bear importantly on understanding the processes of galaxy formation and evolution that deposit chemically enriched material far from galaxies.

Over the past several years, we have been conducting an imaging and spectroscopic survey of faint galaxies in fields of Hubble Space Telescope (HST) spectroscopic target QSOs (Lanzetta et al. 1995; Chen et al. 1998, 2001, hereafter Papers I and II). The goal of the survey is to determine the gaseous extent of galaxies and the origin of QSO absorption systems by directly comparing galaxies and QSO absorption systems along common lines of sight. As a result of the survey, we have so far identified 352 galaxies of apparent magnitude  $m_R < 23$  and redshift  $z < 1.2$ , 230 Ly $\alpha$  absorption systems of redshift  $z < 1.1$ , and 36 C IV absorption systems of redshift  $z < 0.9$  in 24 QSO fields. Impact parameters of the galaxies to the QSO lines of sight range from  $\rho = 10.9$  to  $1576.7 h^{-1}$  kpc. Our galaxy and absorber sample provides for the first time the opportunity to study statistical properties of C IV-absorbing gas around galaxies.

Here we present results of the study. First, we show that C IV absorption systems are strongly clustered around galaxies on velocity scales of  $v \lesssim 250$  km s $^{-1}$  and impact parameter scales of  $\rho \lesssim 100 h^{-1}$  kpc but not on larger velocity or impact parameter scales. This demonstrates that C IV absorption systems are associated with galaxies and strongly suggests that C IV-absorbing gas generally arises in individual galaxies, rather than in a diffuse medium that is loosely associated with galaxy groups, clusters, or other large-scale structures. Next, adopting measurements of galaxy properties presented in Papers I and II (which include  $B$ -band luminosity, surface brightness, and disk-to-bulge ratio), we examine

how properties of the C IV absorption systems depend on properties of the galaxies. On the basis of 14 galaxy and absorber pairs and 36 galaxies that do not produce corresponding C IV absorption lines to within sensitive upper limits, we find that: (1) Galaxies of a range of morphological type and luminosity appear to possess extended C IV gaseous envelopes of radius  $R \approx 100 h^{-1}$  kpc, with abrupt boundaries between the C IV absorbing and non-absorbing regions. (2) The extent of C IV-absorbing gas around galaxies scales with galaxy  $B$ -band luminosity as  $R \propto L_B^{0.5 \pm 0.1}$  but does not depend strongly on galaxy surface brightness, redshift, or morphological type. And (3) the covering factor of C IV clouds within  $\approx 100 h^{-1}$  kpc of galaxies is nearly unity, but there is a large scatter in the mean number of clouds encountered along the line of sight. After scaling to the luminosity of an  $L_*$  galaxy, we find that 13 of 14 galaxies of impact parameter  $\rho < 100 h^{-1}$  kpc are associated with corresponding C IV absorption lines, while only one of 36 galaxies of impact parameter  $\rho > 100 h^{-1}$  kpc are associated with corresponding C IV absorption lines.

Our results indicate that galaxies of a wide range of luminosity and morphological type are surrounded by chemically enriched gas that extends for at least  $\approx 100 h^{-1}$  kpc. Given such a large extent, we consider it unlikely that the absorbing clouds were ejected from the primary galaxies by stellar winds or galactic fountains. Rather, we conclude that the absorbing clouds were probably produced at large galactic radii by either Population III stars or by progressive accretion of gas from surrounding satellite galaxies. If the clouds were formed by satellite accretion, then the abrupt boundaries between the C IV absorbing and non-absorbing regions suggest that galaxies form through dissipational accretion, and the lack of a strong redshift dependence of the extent of C IV-absorbing gas around galaxies suggests that the typical separation between satellites and primary galaxies is larger than  $100 h^{-1}$  kpc. We adopt a standard Friedmann cosmology of dimensionless Hubble constant  $h = H_0/(100 \text{ km s}^{-1} \text{ Mpc}^{-1})$  and deceleration parameter  $q_0 = 0.5$  throughout.

## 2. DATA

The analysis is based on observations of our ongoing imaging and spectroscopic survey of faint galaxies in fields of HST spectroscopic target QSOs (Lanzetta et al. 1995; Papers I and II; Lanzetta et al. 2001 in preparation). As a result of the survey, we have so far identified 352 galaxies of apparent magnitude  $m_R < 23$  and redshift  $z < 1.2$ , 230 Ly $\alpha$  absorption systems of redshift  $z < 1.1$ , and 36 C IV absorption systems of redshift  $z < 0.9$  in 24 QSO fields. Impact parameters of the galaxies to the QSO lines of sight range from  $\rho = 10.9$  to  $1576.7 h^{-1}$  kpc.

Using the Hubble Space Telescope with the Wide Field and Planetary Camera 2, we

have also obtained high-quality optical-wavelength images of 142 of the galaxies in 19 fields, which we have used to measure galaxy  $B$ -band luminosity, effective radius, surface brightness, inclination and orientation of the disk component, axial ratio of the bulge component, and disk-to-bulge ratio by means of a two-dimensional surface brightness profile analysis. These measurements are described and presented in Papers I and II.

### 3. ANALYSIS

In this section, we examine how properties of the C IV absorption systems depend on properties of the galaxies.

#### 3.1. The Galaxy–C IV Absorber Cross-Correlation Function

To establish the statistical relationship between galaxies and C IV absorption systems, we measured the galaxy–C IV absorber cross-correlation function  $\xi_{\text{ga}}(v, \rho)$  as it depends on line-of-sight velocity separation  $v$  and impact parameter separation  $\rho$ . Figure 1 shows  $\xi_{\text{ga}}(v, \rho)$  determined from 352 galaxies and 36 C IV absorption systems. The bin size in velocity separation is  $250 \text{ km s}^{-1}$ , and the bin size in impact parameter separation is indicated in each panel. A total of 563 galaxy and absorber pairs enter into the analysis, of which 153 are of impact parameter separation  $\rho < 100 h^{-1} \text{ kpc}$ , 148 are of  $100 < \rho < 200 h^{-1} \text{ kpc}$ , and 262 are of  $\rho > 200 h^{-1} \text{ kpc}$ . Error bars indicate  $1 \sigma$  Poisson counting fluctuations.

Figure 1 indicates a statistically significant excess of galaxy and C IV absorber pairs at velocity separations  $v \lesssim 250 \text{ km s}^{-1}$  and impact parameter separations  $\rho \lesssim 100 h^{-1} \text{ kpc}$ , but no excess at larger velocities or impact parameters. Specifically, the bin spanning  $v < 250 \text{ km s}^{-1}$  and  $\rho < 100 h^{-1} \text{ kpc}$  is expected to contain  $0.82 \pm 1.34$  pairs but is observed to contain 9 pairs, which indicates that the excess is established at the  $6.1\sigma$  level of significance. The strong signal on small velocity and impact parameter scales demonstrates that C IV absorption systems are associated with galaxies. Further, the lack of signal on larger velocity and impact parameter scales strongly suggests that C IV-absorbing gas generally arises in individual galaxies, rather than in a diffuse medium that is loosely associated with galaxy groups, clusters, or other large-scale structures.

### 3.2. Galaxy and C IV Absorber Pair Sample

To identify galaxy and absorber pairs that are likely to be physically associated with each other, we followed procedures similar to those described in Paper I. First, we considered a galaxy and absorber pair of velocity separation  $v$  and impact parameter separation  $\rho$  to be physically associated if  $\xi_{\text{ga}}(v, \rho) > 1$ . In cases where more than one galaxy could be paired with one absorber under this criterion, we chose the galaxy of smallest impact parameter to form the pair. Next, we excluded galaxy and absorber pairs within  $3000 \text{ km s}^{-1}$  of the background QSOs (because such galaxies and absorbers are likely to be associated with the QSOs). Finally, we measured  $3\sigma$  upper limits to absorption equivalent widths of galaxies that are not paired with corresponding absorbers, retaining only those measurements with  $3\sigma$  upper limits satisfying  $W < 0.3 \text{ \AA}$ . Following these procedures, we identified 14 galaxy and C IV absorber pairs and 36 galaxies that do not produce corresponding C IV absorption to within sensitive upper limits. Redshifts of the galaxy and absorber pairs range from  $z = 0.1242$  to  $0.8920$  with a median of  $\text{med}(z) = 0.3905$ , and impact parameters of the galaxy and absorber pairs range from  $\rho = 12.4$  to  $142.9 h^{-1} \text{ kpc}$  with a median of  $\text{med}(\rho) = 52.6 h^{-1} \text{ kpc}$ . The  $B$ -band luminosities of the galaxies range from  $L_B = 0.03$  to  $2.5 L_{B*}$ . A complete list of the measured properties of the galaxies and C IV absorbers is presented in Paper II.

### 3.3. The Extent of C IV-Absorbing Gas Around Galaxies

To determine the extent of C IV-absorbing gas around galaxies, we examined the relationship between rest-frame C IV  $\lambda 1548$  equivalent width  $W$  and galaxy impact parameter  $\rho$ . Figure 2 shows  $W$  versus  $\rho$  for the 14 galaxy and absorber pairs and the 36 galaxies that do not produce corresponding C IV absorption to within sensitive upper limits. Circles represent early-type elliptical or S0 galaxies, triangles represent early-type spiral galaxies, and squares represent late-type spiral galaxies. Galaxy morphology is determined on the basis of the integrated light ratio of the disk and bulge surface brightness profiles, as described in Papers I and II. Open points with arrows indicate  $3\sigma$  upper limits to  $W$  for galaxies that do not produce corresponding C IV absorption lines.

Figure 2 exhibits three interesting points: First, 12 of 18 galaxies (67%) of impact parameter  $\rho < 70 h^{-1} \text{ kpc}$  are associated with corresponding C IV absorption lines, while only two of 32 galaxies (6%) of impact parameter  $\rho > 70 h^{-1} \text{ kpc}$  are associated with corresponding C IV absorption lines. Evidently, there are abrupt boundaries between the C IV absorbing and non-absorbing regions of galaxies. Second, unlike the situation for Mg II- and Ly $\alpha$ -absorbing gas around galaxies, there is no clear trend for rest-frame equivalent width  $W$  to be progressively stronger at smaller impact parameter  $\rho$ . Third, galaxies associated

with corresponding C IV absorption lines span a wide range of morphological type and luminosity. Specifically, two of the 14 absorbing galaxies are elliptical or S0 galaxies and 12 are spiral galaxies, and three of the 14 absorbing galaxies are of luminosity  $L_B > L_{B*}$ , seven are of  $0.5L_{B*} < L_B < L_{B*}$ , and four are of  $L_B < 0.5L_{B*}$ . Apparently, galaxies of a range of morphological type and luminosity possess extended C IV gaseous envelopes of radius  $R \approx 100 h^{-1}$  kpc, with abrupt boundaries between the C IV absorbing and non-absorbing regions.

### 3.4. The Relationship between Properties of C IV Absorption Systems and Properties of Galaxies

To determine how properties of the C IV absorption systems depend on properties of the galaxies, we examined the relationship between rest-frame C IV  $\lambda 1548$  equivalent width  $W$  and galaxy impact parameter  $\rho$  scaling for various properties (luminosity, surface brightness, and redshift) of the galaxies. Motivated by the apparent abrupt boundary between the C IV absorbing and non-absorbing regions and the apparent lack of a  $W$  versus  $\rho$  anti-correlation described in § 2.3, we modeled the distribution of C IV clouds in the extended gaseous envelopes of galaxies by uniform spheres of radius that depends on some property of the galaxy. Then the number  $n$  of C IV-absorbing clouds intercepted along the line of sight is proportional to the path length through the sphere:

$$n = 2l_0[R^2(x) - \rho^2]^{1/2}, \quad (1)$$

where  $l_0$  is the number density per unit length of the clouds,  $R$  is the radius of the sphere, and  $x$  is some property of the galaxy. Because C IV equivalent width is correlated with the number of individual absorbing components intercepted along the line of sight (Wolfe 1986; York et al. 1986; Petitjean & Bergeron 1994), we take  $W = nk$ , where  $k$  is the equivalent width of a typical absorbing component. Combining equations (1) and (2), the C IV equivalent width  $W$  expected at impact parameter  $\rho$  is given by

$$W = \begin{cases} 2kl_0[R^2(x) - \rho^2]^{1/2} & \rho \lesssim R(x) \\ 0 & \rho \gtrsim R(x), \end{cases} \quad (2)$$

as a function of some property of the galaxy  $x$ .

First, we established a fiducial fit of the model described by equation (2) to the observations for the case in which the radius of the sphere does not depend on any property of the galaxy, i.e. for  $R = R_*$ , where  $R_*$  is the absorbing radius of the galaxy. Following procedures described in Paper I and substituting  $W$  for the dependent variable (instead of

log  $W$  as in Paper I), we solved for  $kl_0$ ,  $R_*$ , and the “cosmic scatter”  $\sigma_c$  using a likelihood analysis. The results are summarized in row 1 of Table 1, which lists  $kl_0$ ,  $R_*$ ,  $\sigma_c$ , and an estimate of goodness of fit  $\chi_\nu^2$  that is equivalent to a reduced  $\chi^2$  with upper limits properly taken into account.

Next, we repeated the fitting allowing the radius  $R$  to scale with galaxy  $B$ -band luminosity  $L_B$  as

$$R = R_* \left( \frac{L_B}{L_{B*}} \right)^\alpha, \quad (3)$$

where  $R_*$  is the characteristic absorbing radius of an  $L_*$  galaxy. The results are summarized in row 2 of Table 1. After accounting for galaxy  $B$ -band luminosity,  $\chi_\nu^2$  is significantly improved with respect to the fiducial fit, and

$$\alpha = 0.5 \pm 0.1, \quad (4)$$

which indicates that the dependence between  $R$  and  $L_B$  is established at the  $5\sigma$  level of significance. The characteristic radius is

$$R_* = 95.9 \pm 7.0 h^{-1} \text{ kpc}. \quad (5)$$

This result applies over the  $B$ -band luminosities  $0.03 \lesssim L_B \lesssim 2.5 L_{B*}$  spanned by the observations.

Figure 3 shows  $W$  versus  $\rho$  for the 14 galaxy and absorber pairs and the 36 galaxies that do not produce corresponding C IV absorption to within sensitive upper limits after scaling for galaxy  $B$ -band luminosity. The abrupt boundary between the C IV absorbing and non-absorbing regions is more evident in Figure 3 than in Figure 2. Specifically, after scaling for galaxy  $B$ -band luminosity, 14 of 15 (93%) of galaxies of impact parameter  $\rho < 112 h^{-1}$  kpc are associated with corresponding C IV absorption lines, while *no* galaxies of impact parameter  $\rho > 112 h^{-1}$  kpc produce corresponding C IV absorption to within sensitive upper limits. A likelihood analysis indicates that the covering factor  $\kappa$  of C IV-absorbing gas around galaxies approaches unity at impact parameters  $\rho < 112 h^{-1}$  kpc, with a  $1\sigma$  lower bound of  $\langle \epsilon\kappa \rangle = 0.91$ . The solid curve in Figure 3 shows the best-fit uniform sphere model.

Next, we repeated the fitting substituting galaxy surface brightness (at the half-light radius)  $\mu_e$  and redshift  $(1+z)$ , respectively, for galaxy  $B$ -band luminosity. The results are summarized in rows 3 and 4 of Table 1. After accounting for surface brightness or redshift, the scaling exponent  $\alpha$  is indistinguishable from zero, and there is no significant improvement in  $\chi_\nu^2$ . We conclude that the C IV extent of galaxies does not depend strongly on galaxy mean surface brightness or redshift. This result applies over surface brightnesses  $18.2 \lesssim \mu_e \lesssim 25.4$  mag arcsec $^{-2}$  and redshifts  $0.09 \lesssim z \lesssim 0.83$  spanned by the observations.



Results of the likelihood analysis can also be used to estimate the mean number of C IV clouds intercepted along a line of sight through a galaxy. Given our estimates of the cosmic scatter  $\sigma_c$  and the typical absorption equivalent width per absorbing component per unit length  $k l_0$  and assuming Poisson counting statistics, so that  $\sigma_c$  is related to  $k$  by

$$\sigma_c = k(W/k + 1)^{1/2}, \quad (6)$$

we find based on the results presented in row 2 of Table 1 that a line of sight through the center of an  $L_*$  galaxy encounters on average

$$n_0 = 8.2 \pm 3.0 \quad (7)$$

C IV absorbing clouds of equivalent width  $k = 0.13 \text{ \AA}$ .

#### 4. DISCUSSION

The primary results of the analysis are as follows: (1) Galaxies of a range of morphological type and luminosity appear to possess extended C IV gaseous envelopes of radius  $R \approx 100 h^{-1} \text{ kpc}$ , with abrupt boundaries between the CIV absorbing and non-absorbing regions. (2) The extent of C IV-absorbing gas around galaxies scales with galaxy  $B$ -band luminosity as  $R \propto L_B^{0.5 \pm 0.1}$  but does not depend strongly on galaxy surface brightness, redshift, or morphological type. And (3) the covering factor of C IV clouds within  $\approx 100 h^{-1} \text{ kpc}$  of galaxies is nearly unity, but there is a large scatter in the mean number of clouds encountered along the line of sight. Apparently, *galaxies of a wide range of luminosity and morphological type are surrounded by chemically-enriched gas<sup>3</sup> that extends for at least  $\approx 100 h^{-1} \text{ kpc}$ .*

---

<sup>3</sup>It is, however, not clear whether or not the extended gas contains abundant metals. There has been a lack of chemical abundance measurements for low-redshift QSO absorption systems, because such analysis requires high resolution, high sensitivity QSO spectroscopy in the ultraviolet spectral range. The only two existing chemical abundance analyses at redshifts  $z < 1$  are both for absorbers of neutral hydrogen column density  $\log N(\text{H I})(\text{cm}^{-2}) \gtrsim 16.0$  and both systems exhibit chemical abundance that approaches the typical solar values (Bergeron et al. 1994; Chen & Prochaska 2000). These measurements, however, cannot be considered representative of the majority of QSO absorption systems at low redshifts, because of an apparent selection bias. Because observations of QSO absorption systems at high redshifts show a wide range of metallicity, we believe that QSO absorption systems at low redshifts also have a range of metallicity. The absorbers in our sample have been identified from random lines of sight. We therefore expect that statistical properties of the absorbers in our sample are comparable to statistical properties of all low-redshift QSO absorption systems. Namely, there exists a range of chemical abundance in our absorber sample.

By combining results of previous studies of extended Mg II, C IV, and Ly $\alpha$  gas around galaxies (derived by analysis of QSO absorption systems), we can establish a schematic picture of the structure of extended gas around galaxies: A typical  $L_*$  galaxy is surrounded by high column density gas of radius a few tens kpc (e.g. van Gorkom 1993), which, because of its high density, remains mostly neutral. The gas becomes gradually ionized as the gas density decreases with increasing galactic radius. Low-ionization species, such as singly ionized magnesium Mg II, become the dominant observational signature out to  $\approx 50 h^{-1}$  kpc (e.g. Bergeron & Boissè 1991). As the density continues to decline at larger galactic radii, the gas becomes still more highly ionized. High-ionization species, such as triply ionized carbon C IV, become the dominant observational signature out to  $\approx 100 h^{-1}$  kpc, at neutral hydrogen column densities  $N(\text{H I}) \approx 10^{16} \text{ cm}^{-2}$  (this paper). The tenuous gas continues to extend to at least  $\approx 180 h^{-1}$  kpc, at neutral hydrogen column densities at least as low as  $N(\text{H I}) \approx 3 \times 10^{14} \text{ cm}^{-2}$  (Papers I and II). This picture applies to galaxies of a wide range of luminosity and morphological type.

Establishing the origin of the chemically enriched gas at large galactic radii is important for understanding the processes of galaxy formation and evolution that deposit chemically enriched material far from galaxies. Here we consider two possible scenarios for the origin of this gas: (1) that the gas is driven out of the galaxies by strong galactic winds and (2) that the gas was produced at large galactic radii.

In the first scenario (which is known as the galactic fountain model), hot gas is brought to large galactic distances by violent supernova explosions, forms cold clouds through subsequent radiative cooling, and falls back to the center of the galaxy (Corbelli & Salpeter 1988). Comparing with the results of our analysis, we find that the galactic fountain model is unlikely to account for extended C IV gas around galaxies for the following reasons: First, hot gas driven by supernova explosion can reach to at most  $\approx 20$  kpc (e.g. Corbelli & Salpeter 1988) before it completely escapes the galaxy, but our analysis indicates that C IV-absorbing gas extends to  $\approx 100 h^{-1}$  kpc. Second, the supernova explosion rate varies significantly between galaxies of different morphological types, but our analysis suggests that galaxies of all morphological types possess extended C IV-absorbing gas to large radii. Third, given a fixed initial flow speed, the ejected gas may reach larger galactic radii from within smaller galaxies, which is at odds with the scaling relation of our analysis that the C IV gaseous extent increases with galaxy luminosity.

In the second scenario, chemically enriched gas is deposited at large radii either by the first generation stars (Population III) or through progressive accretion of gas from surrounding satellite galaxies. But because the pregalactic enrichment due to Population III stars is strongly constrained by the metallicity of Population II stars to be less than  $Z \approx 10^{-3}$

(Carr, Bond, & Arnett 1984) and because observations show that there is already a wide range of metallicity in high-redshift QSO absorption systems (e.g. Rauch 1998), we conclude that Population III stars cannot explain all of the C IV absorbing clouds at large radii, although they may contribute to some of them. On the other hand, theoretical analysis of an accreting satellite model has shown that chemically enriched gas may be stripped out of the surrounding satellites through tidal interaction or may be ejected from the satellites due to supernova explosions to form absorbing clouds at large radii of the primary galaxy (Wang 1993). Supporting evidence is found from observations of nearby spiral galaxies, which shows that there exists at least one satellite around each Milky Way type galaxy (Zaritsky et al. 1993). In addition, H I 21 cm analysis of local dwarf spheroidals suggests that the presence of satellite galaxies may contribute to extended gas in galactic halos (Blitz & Robishaw 2000).

We believe that it is therefore likely that accreting satellites may account for chemically enriched gas at large galactic distances, which has implications for the dynamics of absorbing gas clouds as follows:

First, for an isothermal sphere, the density of accreted gas decreases with radius  $R^{-2}$ . But because of dissipational collisions, absorbing clouds may gradually lose angular momentum during the cooling process and spiral down to the primary galaxies, causing the density of accreted gas to fall off more rapidly than  $R^{-2}$  (Silk & Norman 1981). It appears that the abrupt boundary between the C IV absorbing and non-absorbing regions apparent in Figure 3 supports a sharp steepening in the number density of C IV-absorbing clouds in the outer gaseous envelopes of galaxies. Fitting  $W$  versus  $\rho$  of Figure 3 with a single power-law model  $W \propto \rho^\alpha$  yields  $\alpha = -1.45 \pm 0.18$ , which implies a density distribution  $R^{-2.45 \pm 0.18}$  (see Lanzetta & Bowen 1990). The dotted line in Figure 3 shows the best-fit power-law model. We conclude that the abrupt boundaries the C IV absorbing and non-absorbing regions of galaxies is indicative of dissipational formation processes of galaxies.

Second, our results indicate that the extent of C IV-absorbing gas does not depend strongly on galaxy redshift, which implies that C IV gaseous envelopes of galaxies are essentially static over a large cosmic time interval. Given our estimate in Equation (7) of the average number of clouds along a line of sight through the center of an  $L_*$  galaxy and adopting a velocity dispersion  $v \approx 200 \text{ km s}^{-1}$  of a typical  $L_*$  galaxy, we estimate that the collision time between C IV-absorbing clouds is  $t_{\text{coll}} \approx 2R_*/(n_0v) \approx 1.1 \times 10^8 \text{ yr}$ . In comparison, the dynamical time for the clouds to fall through the gravitational potential of a galaxy is  $t_{\text{dyn}} \approx \pi R_*/2v \approx 7.4 \times 10^8 \text{ yr}$ . Unless the gaseous envelopes of galaxies are continually supplied with matter or energy, it is clear that the accreted gas clouds will rapidly decay to lower orbits, resulting in smaller gaseous cross sections with time. This directly contradicts our observations. A solution to this problem may be that satellites at

large galactic radii provide a constant supply of fresh gas. We therefore conclude that if C IV-absorbing clouds are formed through dissipational accretion of gas from surrounding satellites, the mean separation between the satellites and the primary galaxies may be larger than  $100 h^{-1}$  kpc.

This work was supported by STScI grant GO-07290.01-96A and NSF grant AST-9624216.

## REFERENCES

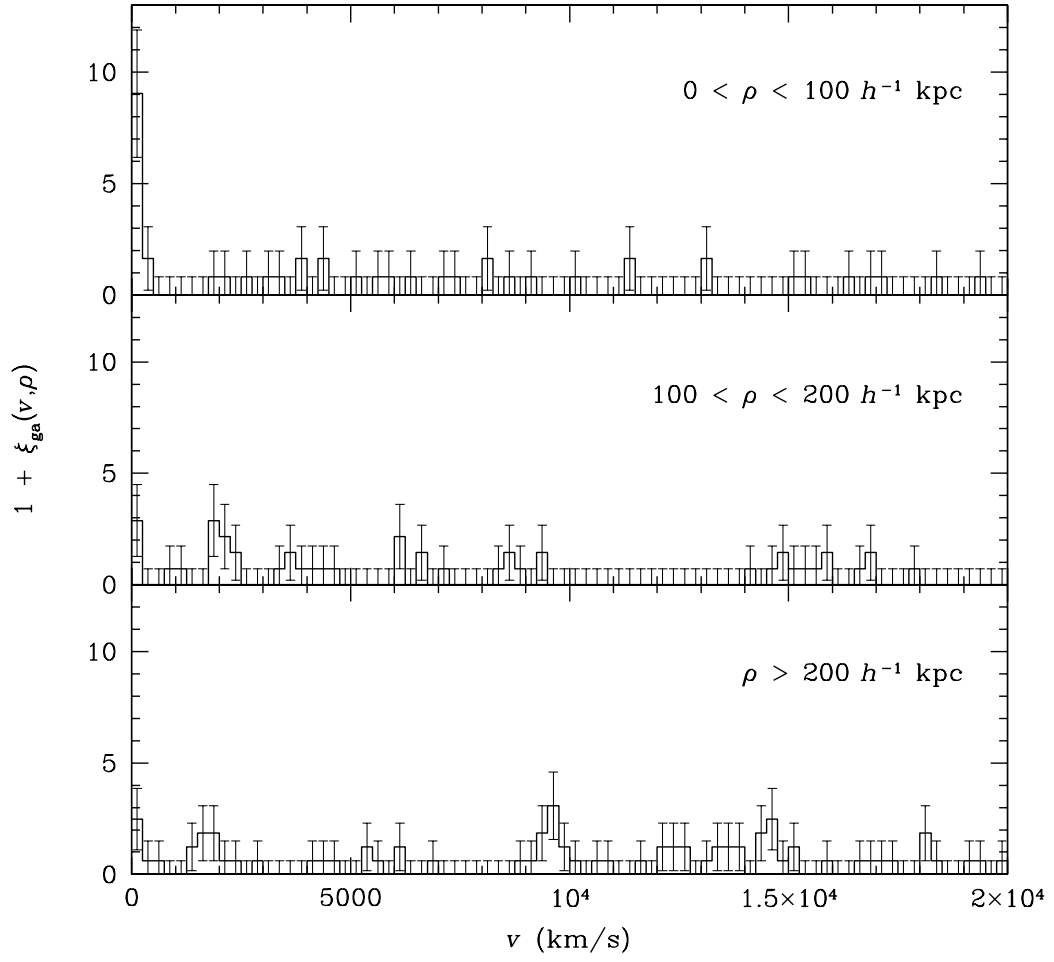
- Bergeron, J. & Stasińska, G. 1986, *A&A*, 169, 1
- Bergeron, J. & Boissé, P. 1991, *A&A*, 243, 344
- Bergeron, J. et al. 1994, *ApJ*, 436, 33
- Blitz, L. & Robishaw, T. 2000, *ApJ*, 541, 675
- Carr, B. J., Bond, J. R., & Arnett, W. D. 1984, *ApJ*, 277, 445
- Chen, H.-W., Lanzetta, K. M., Webb, J. K., & Barcons, X. 1998, *ApJ*, 498, 77 (Paper I)  
\_\_\_\_\_. 2001, *ApJ* submitted (Paper II)
- Chen, H.-W. & Prochaska, J. X. 2000, *ApJ*, 543, L9
- Churchill, C. W., Mellon, R. R., Charlton, J. C., Jannuzi, B. T., Kirhakos, S., Steidel, C. C., & Schneider, D. P. 1999, *ApJ*, 519, L43
- Corbelli, E. & Salpeter, E. E. 1988, *ApJ*, 326, 551
- Lanzetta, K. M. & Bowen, D. V. 1990, *ApJ*, 357, 321
- Lanzetta, K. M. & Bowen, D. V. 1992, *ApJ*, 391, 48
- Lanzetta, K. M., Bowen, D. V., Tytler, D., & Webb, J. K. 1995, *ApJ*, 442, 538
- Petitjean, P. & Bergeron, J. 1994, *A&A*, 283, 759
- Rauch, M. 1998, *ARA&A*, 36, 267
- Silk, J. & Norman, C. 1981, *ApJ*, 247, 59
- Steidel, C. C. 1993, in *The Evolution of Galaxies and Their Environmen*, Proc. 3d Tetons Summer Astrophysics Conference, ed. J. M. Shull & H. A. Thronsons, Jr., p. 263
- Steidel, C. C., Dickinson, M., Meyer, D. M., Adelberger, K. L., & Sembach, K. R., 1997, *ApJ*, 480, 568
- van Gorkom, J. 1993, in *The Evolution of Galaxies and Their Environmen*, Proc. 3d Tetons Summer Astrophysics Conference, ed. J. M. Shull & H. A. Thronsons, Jr., p. 345
- Wang, B. 1993, *ApJ*, 415, 174
- Wolfe, A. M. 1983, *ApJ*, 268, L1
- Wolfe, A. M. 1986, in *Proc. NRAO Conf. on Gaseous Halos of Galaxies*, ed. J. Bregman and J. Lockman (Green Bank: NRAO), P. 259
- York, D. G., Dopita, M., Green, R., & Bechtold, J. 1986, *ApJ*, 311, 610

Zaritsky, D., Smith, R., Frenk, C. & White, S. D. M. 1993, ApJ, 405, 464

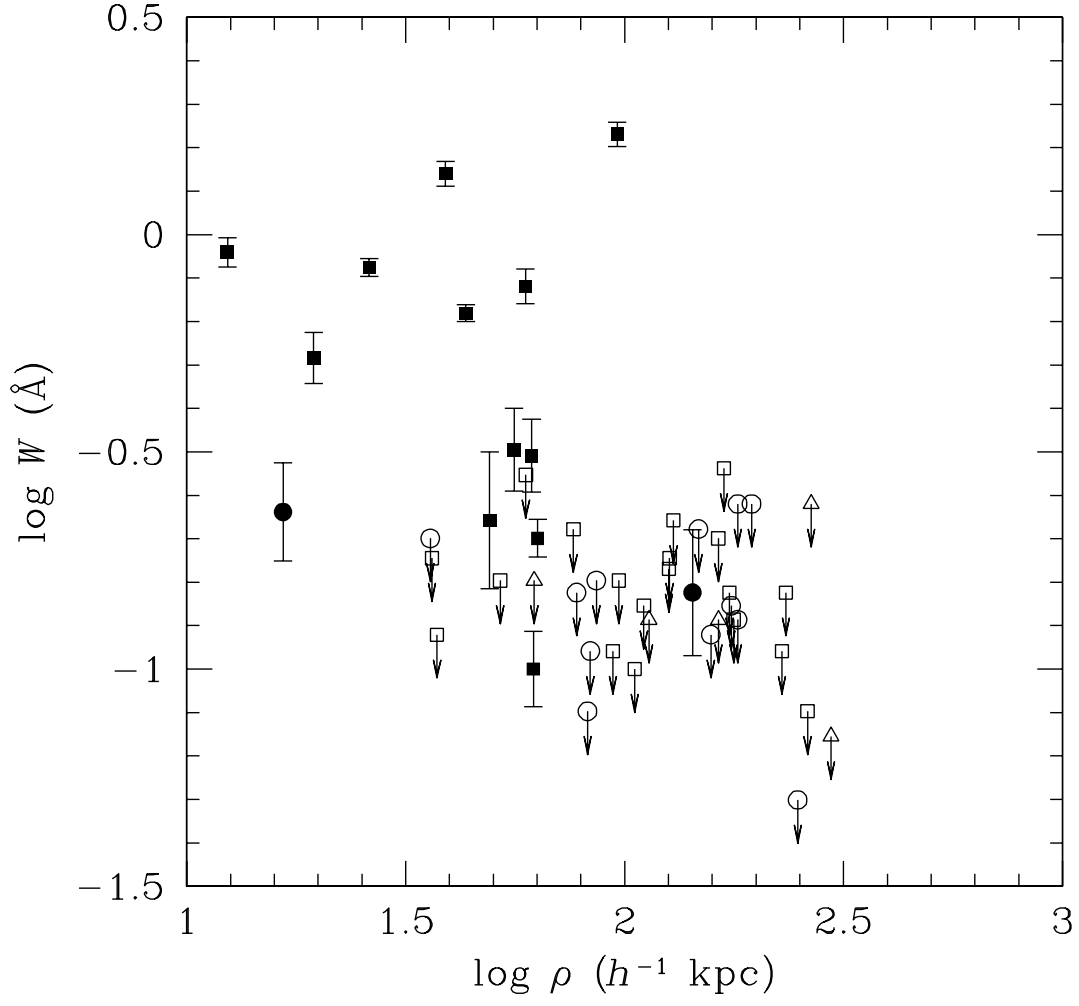
Fig. 1.— Galaxy–C IV absorber cross-correlation function  $\xi_{ga}(v, \rho)$  vs. velocity separation  $v$  and impact parameter separation  $\rho$ . The bin size in velocity separation is  $250 \text{ km s}^{-1}$ . The bin size in impact parameter separation is  $100 h^{-1} \text{ kpc}$ . Error bars indicate  $1 \sigma$  Poisson counting errors.

Fig. 2.— Logarithm of C IV rest-frame equivalent width  $W$  vs. logarithm of galaxy impact parameter  $\rho$ . Circles represent early-type elliptical or S0 galaxies, triangles represent early-type spiral galaxies, and squares represent late-type spiral galaxies. Closed points indicate detections. Open points with arrows indicate  $3\sigma$  upper limits of non detections.

Fig. 3.— Logarithm of C IV rest-frame equivalent width  $W$  vs. logarithm of galaxy impact parameter  $\rho$  scaled by galaxy  $B$ -band luminosity. The scaling factor is determined from the analysis described in § 3.4. Symbols represent the same as those in Figure 2. The solid curve indicates a uniform sphere model that best fits the data. The dotted line indicates the best-fit power-law model to the data.







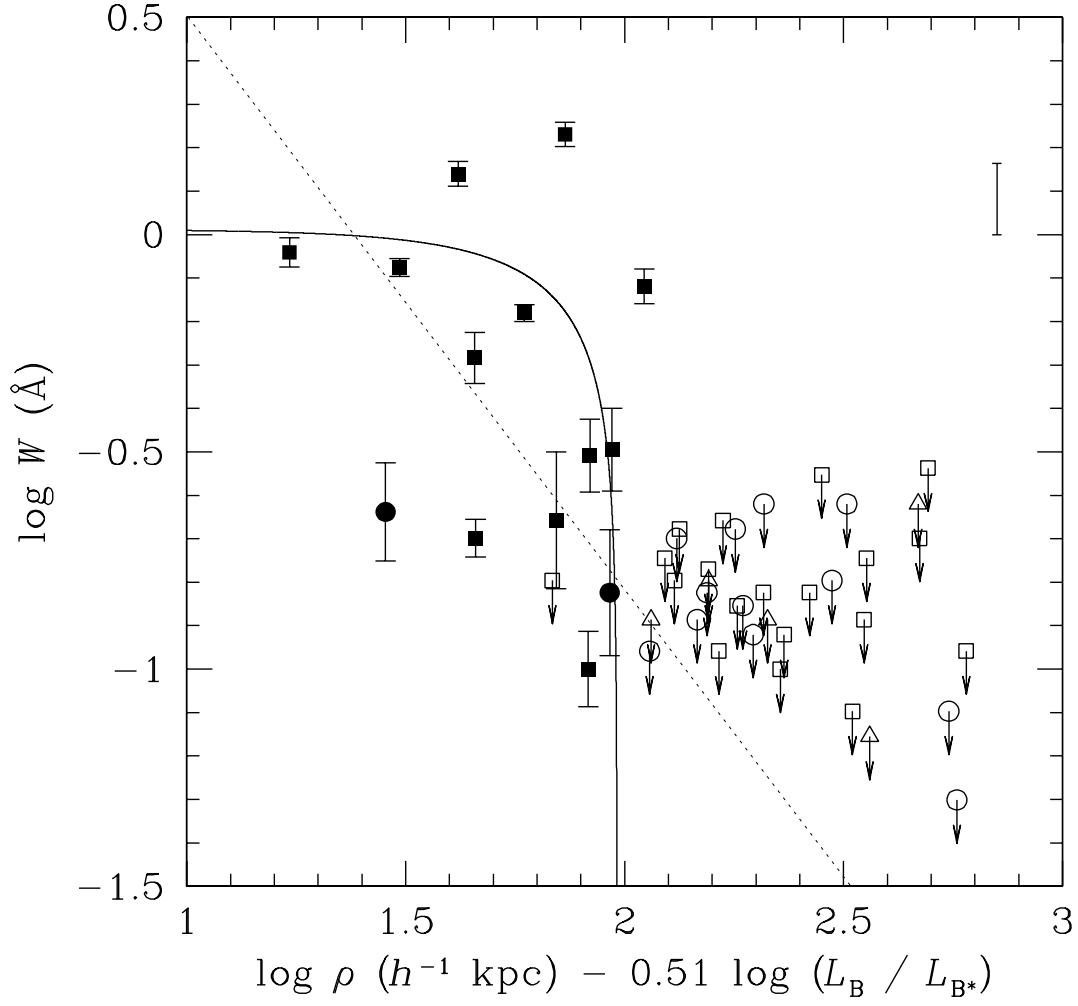


Table 1  
Results of Likelihood Analysis

Measurements	$kl_0$	$R_*$	$\alpha$	$\sigma_c$	$\chi_\nu^2$
1. $W - \rho$ .....	$0.005 \pm 0.001$	$64.0 \pm 2.4$	...	0.23	2.9
2. $W - \rho - L_B$ .....	$0.006 \pm 0.001$	$95.9 \pm 7.0$	$0.5 \pm 0.1$	0.39	1.2
3. $W - \rho - \mu_e$ .....	$0.004 \pm 0.001$	$66.2 \pm 4.0$	$0.04 \pm 0.05$	0.25	2.7
4. $W - \rho - (1 + z)$ .....	$0.005 \pm 0.002$	$60.0 \pm 3.0$	$0.4 \pm 0.7$	0.29	2.7